Continental lithosphere folding in central Asia (Part II): Constraints from gravity and tectonic modelling

Burov, E.B.; Nikishin, A.; Cloetingh, S.A.P.L.; Lobkovsky, L.I.

published in
Tectonophysics
1993

document version
Publisher's PDF, also known as Version of record

Tectonophysics, 226 (1993) 73–87
Elsevier Science Publishers B.V., Amsterdam

Continental lithosphere folding in Central Asia (Part II): constraints from gravity and topography

E.B. Burov [a,b]*, L.I. Lobkovsky [c], S. Cloetingh [d]** and A.M. Nikishin [e]

[a] *Department of Earth Sciences / GETECH, University of Leeds, Leeds LS2 9JT, England*
[b] *Institute of Physics of the Earth, Russian Academy of Sciences, Moscow, Russia*
[c] *Russian Institute of Oceanology of Russian Academy of Sciences, Moscow, Russia*
[d] *Institute of Earth Sciences, Vrije Universiteit, Amsterdam, The Netherlands*
[e] *Department of Geology, Moscow State University, Moscow, Russia.*

(Received November 24, 1992; revised version accepted April 27, 1993)

ABSTRACT

Periodical sub-parallel fold-like structures observed in the Western Gobi have two characteristic dominant wavelengths of approximately 50 and 300–360 km. We explain these observations in terms of independent quasi-viscous folding of the crustal and upper-mantle parts of the lithosphere due to horizontal transpressional stresses in Central Asia induced by the collision with the Indian plate. We derive a model for the mechanical response of the continental lithosphere to horizontal stresses for a rheologically-layered plate with non-Newtonian power law rheology overlying a low-viscosity asthenosphere. The differentiation in the effective viscosity and thickness of the strong upper-crust and upper-mantle lithosphere, along with the presence of a low-viscosity lower crust between them, leads to their partial decoupling during compressional deformation. These features result in the appearance of different wavelengths of the folds in the Western Gobi region. We derive simple semi-analytical estimates for the dominant wavelengths and rates of growth of surface undulations, constrained by data from experimental rock mechanics, topography, and gravity.

Introduction

Observation, theory, and experiments demonstrate a feedback between loads and forces on the continental plates and their mechanical properties (e.g. Kirby, 1983, 1985; Kusznir and Karner, 1985). Recent studies of the structure of the lithosphere have shown that it is significantly non-uniform at least in vertical direction and, therefore, can be stratified into several rheological zones (quasi-layers) with essentially different mechanical properties. Models for the layered rheology of the oceanic lithosphere account for non-uniform mechanical properties by the introduction of a 3-layer (brittle–elastic–plastic) yield-stress envelope analogue to that formulated by Goetze and Evans (1979) and McNutt and Menard (1982) and initially applied primarily to oceanic lithosphere (McAdoo et al., 1985; Chamot-Rooke and Le Pichon, 1989).

In most cases the crust is ignored in models of the mechanical behaviour of the oceanic lithosphere, as its thickness is small in comparison with the total thickness of the lithosphere. In contrast, the crust contributes almost half of the total thickness of continental lithosphere and, consequently, cannot be neglected. The mechanical properties of crustal rocks are essentially different from those of mantle rocks (the lower crust is much weaker than the overlying upper crust and underlying upper mantle lithosphere; the existence of the low-strength layer between the stronger ones can provide decoupling levels). This separation is caused mainly by the difference in flow laws for the crustal and mantle rocks. The crustal part of the continental lithosphere is characterised by the flow law of quartz- (diabase-,

* *Present address*: Institut de Physique du Globe de Paris, 4 Place Jussieu, 75252 Paris, France.
** Corresponding author.

diorite-) rich rocks having lower temperature of creep activation than of olivine-dominated mantle (Ranalli and Murphy, 1987). Quartz, with properties constraining the lower mechanical boundary of the strength of the crustal rocks (Brace and Kohlstedt, 1980; Tsenn and Carter, 1987), is weak at temperature–pressure conditions corresponding to depths from 10–15 to 20–35 km, whereas mantle olivine can be strong to depths of the order of 100 km for the old continental lithosphere (see Fig. 1). Correspondingly, the lower boundary of the mechanically strong upper crust can be considerably shallower than the Moho which presents in itself a major rheological discontinuity (Figs. 1 and 3). Therefore, the interval located between these two boundaries is relatively weak, thus forming a viscous channel separating the upper crust and mantle

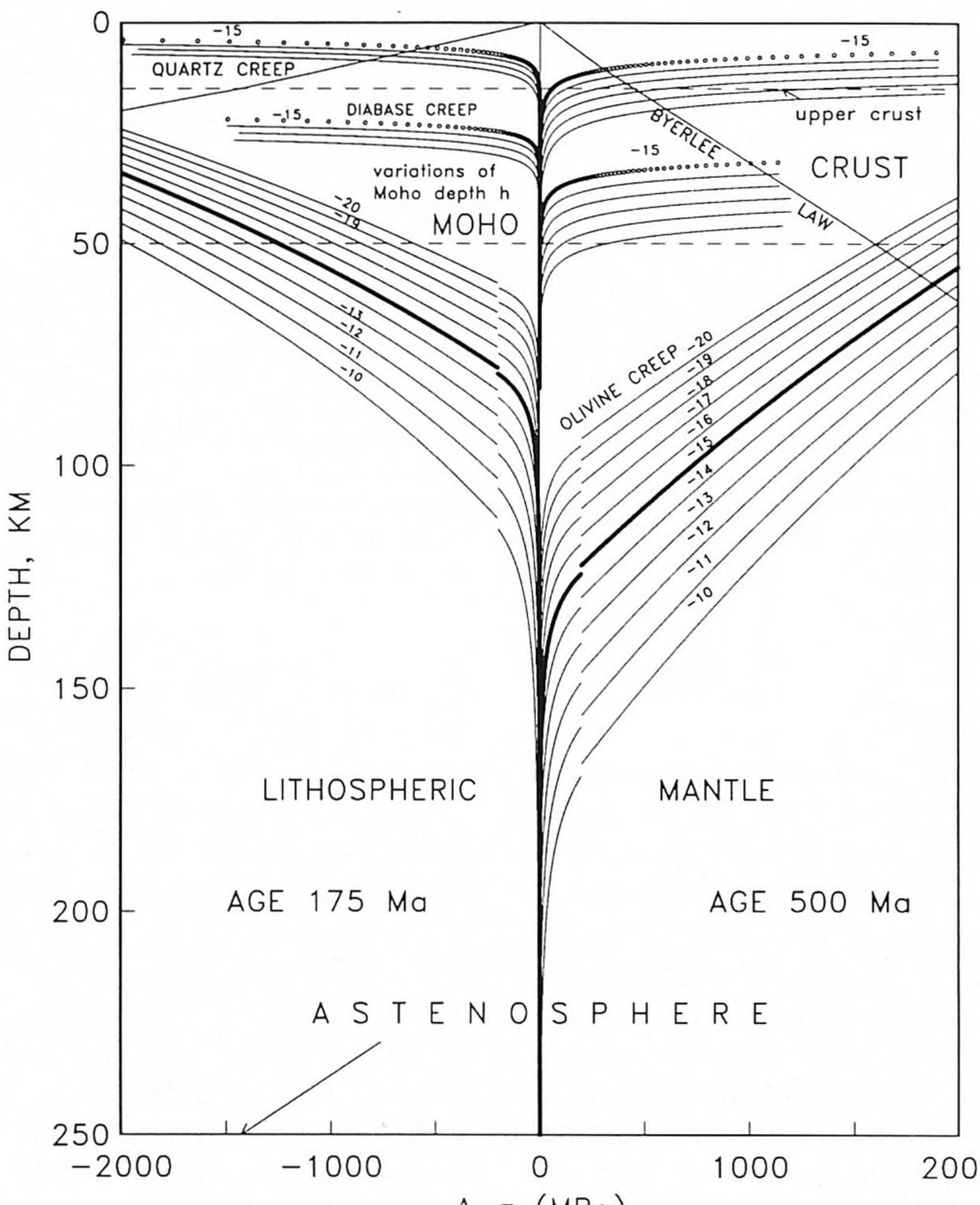

Fig. 1. Yield-stress envelope for continental lithosphere. The right-hand side of the envelope (tension) is computed for a typical case of thermal age 500 Ma, strain rate $\dot{\epsilon} \sim 3 \times 10^{-15}$ s^{-1} (for comparison, the effect of strain rate variation in a range of 10^{-10}–10^{-20}s^{-1} is also shown). The left-hand side of the picture (compression) shows part of the yield-stress envelope for thermally young 175 Ma (e.g. rejuvenated, or re-heated) continental lithosphere. Note that Byerlee's law of brittle failure is practically age/temperature independent, but there is a strong difference (asymmetry) between the compressional and tensional modes. For the same age the ductile parts of the yield-stress envelope are symmetric for tension and compression. The effective basic viscosity of the material can be estimated from simple relation $\mu_{\text{eff}} = \sigma/2\dot{\epsilon}$. For the Western Gobi we assume: Moho depth $h = 50$ km, average surface heat flow of 60 mW m^{-2} (after Burov and Diament, 1992).

lithosphere (Chen and Molnar, 1983; Zoback et al., 1985). This relatively low-viscosity channel can act as a detachment zone between the strong upper crustal level of the lithosphere and the top of the mantle lithosphere (Lobkovsky and Kerchman, 1991). The differential movement between the upper crust, lower crust and the mantle lithosphere can be accompanied by additional heat dissipation and passive movements of the material in the lower crust (Lobkovsky, 1988; Kruse et al., 1991).

This sandwich-like structure of the continental lithosphere potentially gives rise to disharmonic folding at upper crust and mantle levels due to horizontal stresses applied to the margins of plates interacting at intercontinental collision zones (King, 1986; Hall and Chase, 1989; Stein et al., 1989; Stephenson and Cloetingh, 1991). Because of the difference in the effective strength of the levels, the characteristic wavelengths of the folds will be also different. We suggest that this mode of compressional deformation occurs in the region of plate collision in the Western Gobi (Fig. 2; see also Nikishin et al., 1993-this volume). To investigate the way of development of the deformation, we use a mechanical model of viscous folding of the continental lithosphere for this collisional zone (Fig. 3). As discussed in the companion paper (Nikishin et al., 1993-this volume), the neotectonic history of this area (formed in the Late Palaeozoic–Early Mesozoic, and renewed in the Jurassic, Cretaceous and Tertiary) is characterised by the presence of spatially periodical vertical movements of the basement related to the sub-parallel surface structures with dominant wavelengths clustering around 50 and 300–360 km (Fig. 4). The trend of the sub-periodical structures is approximately in a NE direction, roughly coinciding with the direction of northward motion of the Indian sub-continent. The motion of India causes N-NW-NE movement of the Pamir–Tibet and Tarim blocks, apparently responsible for the NW-N-NE orientation of the major horizontal compressional stresses and NE–N–NW orientation of the orthogonal intermediate horizontal transpressional stresses, respectively, observed in Tien Shan and the Western Gobi (Tapponnier and Molnar, 1979). Deformations with a wavelength of 50 km are not associated with the gravity anomalies, but are clearly expressed in the space spectrum of the movements. This supports the notion of upper crust detachment folding, because the deformation of the rheological interface between the upper crust and lower crust is not associated with deformation of density boundaries.

Mechanical properties of the lithosphere

For old continental plates the effective flexural rigidity of the crust is always noticeably less than that of the mantle lithosphere (Kusznir and Karner, 1985; in fact, this may be valid also for young lithosphere). As a result, the overall mechanical strength of the lithosphere is mainly controlled by the mechanical behaviour of the upper mantle levels (De Rito et al., 1986, 1989; McNutt et al., 1988; Burov and Diament, 1992). Burov and Diament (1992) found that for Palaeozoic lithosphere the average effective elastic thickness h_1 for quartz-dominated crust is about 10–20 km, whilst for the mantle lithosphere it is about $\tilde{h}_2 = 40$–65 km ($\tilde{h}_2 = (h_2 - h)$; h_2 is the depth to the lower boundary of the mechanical lithosphere; h is the Moho depth). The effective elastic thickness of the plate, consisting of n detached layers is $h_{\text{eff}} = (\sum_{i=1}^{n} h_i^3)^{1/3}$, where h_i is a effective elastic thickness of i-th layer. Correspondingly, the overall effective elastic thickness h_e of the 2-layer plate is:

$$h_e = \sqrt[3]{h_1^3 + \tilde{h}_2^3} \approx \max(h_1, \tilde{h}_2) = \tilde{h}_2 \qquad (2.1)$$

Although experimentally derived power law relations describe a strongly non-Newtonian behaviour of the materials, an "effective" viscosity can be introduced for ductile domains deforming at basic steady strain rate $\dot{\epsilon}$:

$$\mu_{\text{eff}} = \sigma / 2\dot{\epsilon} \qquad (2.2a)$$

For most lithospheric materials in creep mode $\dot{\epsilon} = A^* \sigma^n \exp[-H^*/(RT)]$ (Kirby and Kronenberg, 1987; Mackwell et al., 1990), μ_{eff} can be expressed as:

$$\mu_{\text{eff}} = 1/(2A^*)\sigma^{1-n} \exp[H^*/RT)]$$
$$= 1/(2A^{*1/n})\dot{\epsilon}^{-1+1/n} \exp[H^*/(nRT)] \qquad (2.2b)$$

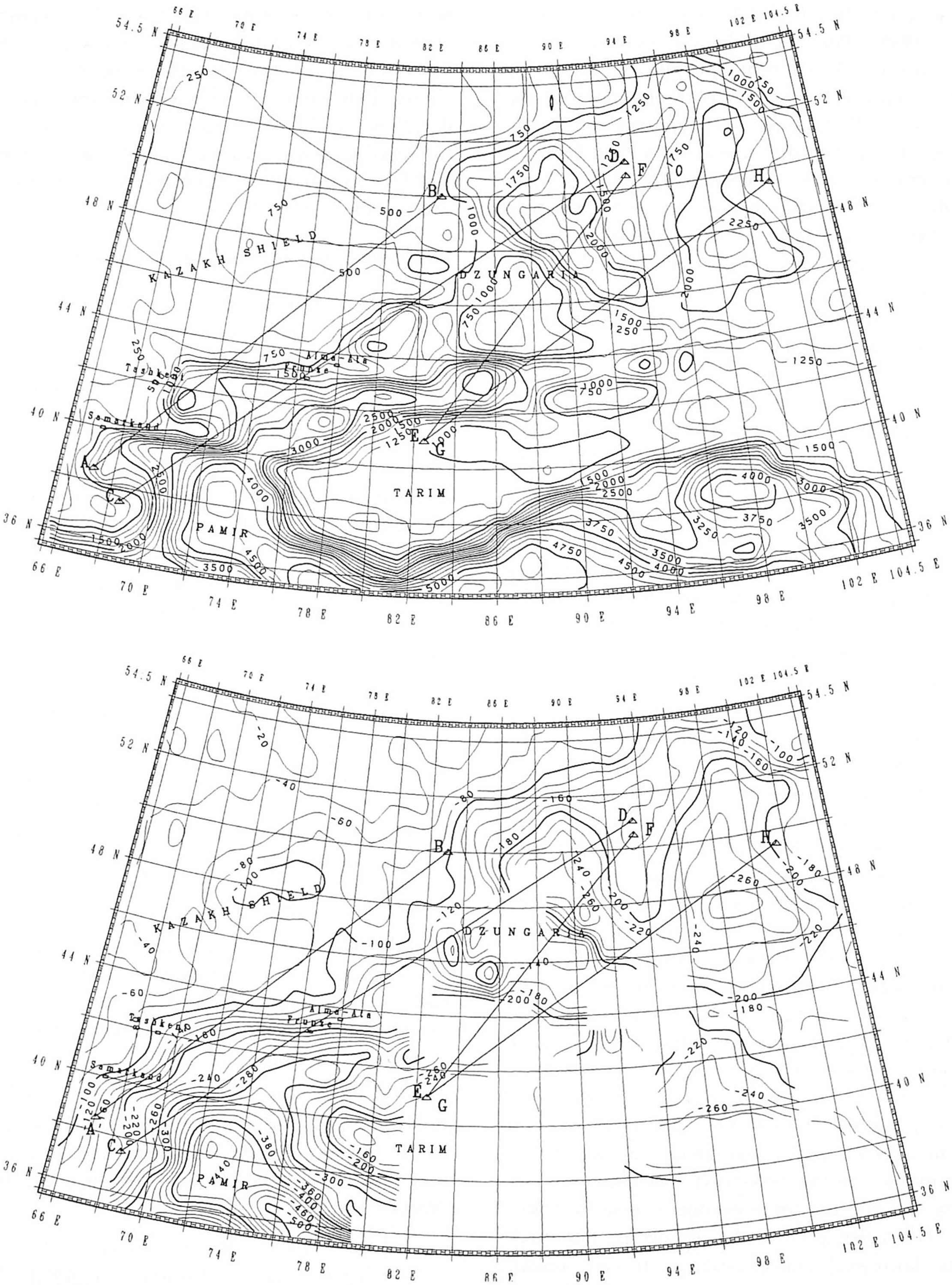

Fig. 2 (a). The map of mean topography elevations ($60' \times 60'$) in Central Asia with the location of data profiles. $60' \times 60'$ data overlapped on the profiles with fine $7.5' \times 5'$ data in the zone between 35.5°N, 75°E–45°N, 80°E. (b). Analogous map of mean Bouguer gravity anomalies.

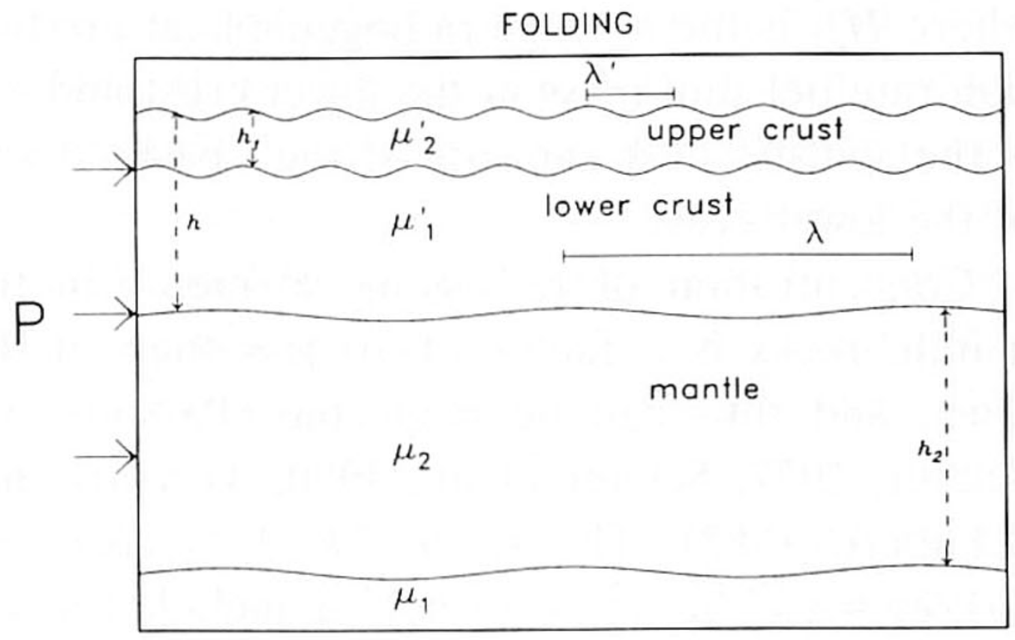

Fig. 3. Cartoon of the model of two-level folding of the continental lithosphere under action of horizontal stress P. Competent crustal and mantle portions of the lithosphere are decoupled by low-viscosity material of the lower crust, and have different effective strengths and viscosities (h_1, $\tilde{h}_2$ and μ'_2, μ_2 respectively). As the result, the deformation has two different dominant wavelengths, λ' and λ. The effective viscosity of the lower crust is μ'_1, and the viscosity of the asthenosphere is μ_1.

where σ is the differential stress; $R = 1.986$ cal (mol K)$^{-1}$ is the gas constant; T is the temperature in K; A^* is the material constant; n is the effective power exponent, ranging from 2 to 4.5 dependent on the mineral; and H^* is the activation enthalpy. For quartz-dominated rocks we assume $A^* = 5 \times 10^{-12}$ (Pa s)$^{-1}$, $H^* = 45$ kcal mol^{-1}, $n = 3$ (Brace and Kohlstedt, 1980). For dry olivine we use eq. (2.2b) for $\sigma \leqslant 200$ MPa ($A^* = 7 \times 10^{-14}$ (Pa s)$^{-1}$; $H^* = 125$ kcal mol^{-1}; $n = 3$), whilst for $\sigma \geqslant 200$ an approximate form suggested by Molnar and Tapponnier (1981) is more convenient:

$$\mu_{\text{eff}} = 1/(2\dot{\epsilon})\sigma_0\left[1 - \sqrt{\ln(\dot{\epsilon}_0/\dot{\epsilon})RT/E^*}\right] \quad (2.2c)$$

where $\sigma_0 = 8.5 \times 10^3$ MPa, $\dot{\epsilon}_0 = 3 \times 10^{15}$ s^{-1} and $E^* = 128$ kcal mol^{-1}. The average strain rates ($3 \div 6 \times 10^{-15}$ s^{-1}) in Central Asia and Western Gobi are quite steady over the geological time scales (Molnar and Deng Qidong, 1984; see also Nikishin et al., 1993-this volume).

The mechanical behaviour of the lower crust under certain conditions could be controlled by creep laws of rocks with higher activation temperature, than quartz (e.g. Stephenson and Cloetingh, 1991). This could be potentially important in cases where the surface heat flow is relatively low (< 50 mW m^{-2}) and/or Moho is not deeper than 30–35 km (Fadaie and Ranalli, 1990). In the Western Gobi the surface heat flow is exceeding 60 mW m^{-2}, and average Moho depths are about 45–55 km (Burov et al., 1990; Li Fu-Tian et al., 1990). Consequently, a quartz creep law for the whole crust is probably a reasonable approximation. This choice is also justified by the absence

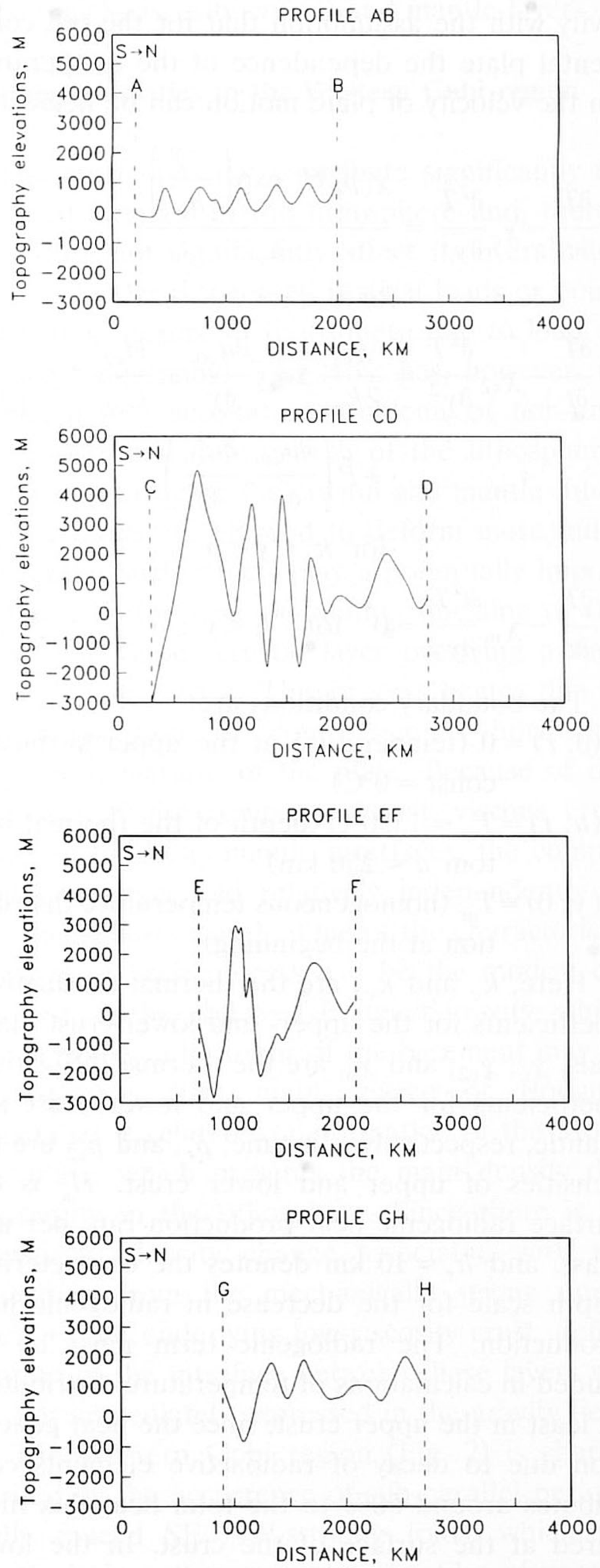

Fig. 4. Neotectonic vertical movements of the basement, along the profiles $A-B$, $C-D$, $G-H$, $E-F$ shown in Fig. 2.

of the lower crust seismicity in this region (Chen and Molnar, 1983; Meissner and Strehlau, 1982) which is to be expected if the lower crust is strong and brittle.

The temperature distribution $T = T(y)$, necessary to estimate the effective viscosity, can be obtained from the equation of the thermoconductivity with the assumption that for the old continental plate the dependence of the temperature on the velocity of plate motion can be neglected:

$$\begin{cases} \dfrac{\partial T}{\partial t} - \chi_c \dfrac{\partial^2 T}{\partial y^2} = \dfrac{\chi_c \rho_c H_s \exp\left(\dfrac{-y}{h_r}\right)}{k_c} \\ \qquad \text{for } 0 \leqslant y \leqslant h_1 \\ \dfrac{\partial T}{\partial t} - \chi_{c2} \dfrac{\partial^2 T}{\partial y^2} = \dfrac{\chi_{c2}}{2k_{c2}} \Delta\sigma_{c2} \dfrac{\partial u_{c0}}{\partial y} + \dfrac{H_{c2}}{C_{c2}} \\ \qquad + \tilde{P}\left(\dfrac{\partial \tilde{u}_{c0}}{\partial y}, \dfrac{\partial \tilde{u}_{c0}}{\partial x}\right) \\ \qquad \text{for } h_1 < y \leqslant h \\ \dfrac{\partial T}{\partial t} - \chi_m \dfrac{\partial^2 T}{\partial y^2} = 0 \quad \text{for} \quad h < y \leqslant a \end{cases} \tag{2.3}$$

The boundary conditions are:

$T(0, t) = 0$ (temperature at the upper surface = const = 0°C)

$T(a, t) = T_m = 1350$°C (depth of the thermal bottom $a \approx 250$ km)

$T(y, 0) = T_m$ (homogeneous temperature distribution at the beginning)

Here, k_c and k_{c2} are the thermal conductivity coefficients for the upper- and lower-crust materials, χ_c, χ_{c2}, and χ_m are the thermal diffusitivity coefficients for the upper and lower crust and mantle, respectively; t is time; ρ_c, and ρ_{c2} are the densities of upper and lower crust, H_s is the surface radiogenic heat production rate per unit mass, and $h_r \approx 10$ km denotes the characteristic depth scale for the decrease in radiogenic heat production. The radiogenic term must be included in calculations of temperature distribution at least in the upper crust, since the heat generation due to decay of radioactive elements contributes around 50% to the total heat flux measured at the surface of the crust. In the lower crust the term $\chi_{c1} k_{c1}^{-1} \rho_{c2} H_s \exp(-y h_r^{-1})$ can be replaced with averaged heat generation $H_{c2} C_{c2}^{-1}$, where H_{c2} is the average radiogenic heat production rate per unit mass in the lower crust and C_{c2} is the specific heat capacity of the "basic" rocks of the lower crust.

Concentration of radiogenic elements in the mantle rocks is a factor of 10 less then in the crust, and thus can be neglected (Parsons and Sclater, 1977; Sclater et al., 1980; Turcotte and Schubert, 1982). The term $(2k_{c2})^{-1} \chi_{c2} \Delta\sigma_{c2} \partial u_{c2}(y)/\partial y \approx \chi k_c^{-1} \tilde{\mu}_2 u_{c0}^2/(h - h_1)^2$ is included to account for dissipative heat generation due to possible viscous sliding between the crustal and mantle portions of the lithosphere; $\tilde{\mu}_2$ is the mean viscosity of crustal material in the viscous channel; u_{c0} is the averaged velocity of differential motion between upper crust and lithospheric mantle. $\tilde{P}(\partial \tilde{u}_{c0}/\partial y, \partial \tilde{u}_{c0}/\partial x)$ is the velocity perturbation term, related to 2-D flow velocity perturbations due to folding. Since these perturbations are assumed to be relatively small, for preliminary calculations it is taken to be zero. The expression for $\tilde{P}$ is:

$$\tilde{P} = \chi_{c2} k_{c2}^{-1} \mu_{c2} \left[4(\psi_{xy})^2 + (\psi_{yy} - \psi_{xx})^2 \right]$$

where ψ_{xy}, ψ_{yy}, ψ_{xx} are second-order partial derivatives of the perturbation stream function derived in the next sections.

The homogeneous solution $T_h(y, t)$ (Carslaw and Jaeger, 1959) is:

$$T_h(y, t) = T_m \left\{ y a^{-1} + \sum_{n=1} A_n \exp\left[-\left(\frac{n\pi}{a}\right)^2 \chi t \right] \sin\left(\frac{n\pi y}{a}\right) \right\}$$

The partial solution T_p is obtained with additional assumption that

$$T\big|_{h_1 - 0} = T\big|_{h_1 + 0}; \quad \left.\frac{\partial T}{\partial y}\right|_{h_1 - 0} = \left.\frac{\partial T}{\partial y}\right|_{h_1 + 0};$$

$$T\big|_{h - 0} = T\big|_{h + 0}; \quad \left.\frac{\partial T}{\partial y}\right|_{h - 0} = \left.\frac{\partial T}{\partial y}\right|_{h + 0}$$

The last boundary condition assumes heat flux continuity across the crust–mantle boundary. Applying the solution $T(y, t) = T_h(y, t) + T_p(y, t)$ of the thermoconductivity equation (2.3) to eqs.

(2.2b,c), we calculated the resulting yield-stress envelope, that is a contour $\sigma_e = f(y)$, within which the lithospheric materials can be competent and outside of which they are weak in terms of characteristic geological time scales (say, the characteristic relaxation time for the competent lithosphere is of order of 10^{-7} yr or more, while that for the weak regions and underlying mantle is about $10^{-4} \div 10^{-5}$ yr (Fig. 1). Therefore we get that the typical relation of the effective viscosity within the yield-stress envelope (contour delineating competent regions of the lithosphere; see Fig. 1) to the effective viscosity of surroundings is about of two or more orders.

The values of the parameters of the thermoconductivity equations used for our calculations, are:

$k_c = 2.5\ \mathrm{Wm^{-1}K^{-1}}$; $k_{c2} = 2\ \mathrm{Wm^{-1}K^{-1}}$; $k_m = 3.5\ \mathrm{Wm^{-1}K^{-1}}$; $\chi_c = 8.3 \times 10^{-7}\mathrm{m^2s^{-1}}$; $\chi_{c2} = 6.7 \times 10^{-7}\mathrm{m^2s^{-1}}$; $\chi_m = 8.75 \times 10^{-7}\mathrm{m^2s^{-1}}$; $\rho_c = 2650\ \mathrm{kg\ m^{-3}}$; $\rho_{c2} = 2900\ \mathrm{kg\ m^{-3}}$; $H_s = 7.5\text{–}9.5 \times 10^{-10}\ \mathrm{W\ kg^{-1}}$; $H_{c2}C_{c2}^{-1} = 1.7 \times 10^{-13}\mathrm{K\ s^{-1}}$.

The average Moho depth in Gobi is around $h = 50$ km (Burov et al., 1990) and an average value of h_2, estimated using eqs. (2.2a–c) and the solution for $T(y, t)$ for Palaeozoic age, is around 120 km; that gives $\tilde{h}_2 \approx 70$ km (Fig. 1). The value of h_1 is approximately $10 \div 15$ km. The estimated typical relation of viscosity of the competent crustal and mantle layers to the viscosity of the surrounding material is thus around μ'_2/μ'_1, $\mu_2/\mu_1 = 10 \div 50$ ($\mu'_2, \mu_2 \sim 10^{22} \div 10^{23}$ Pa × s and $\mu'_1, \mu_1 \sim 10^{21}$ Pa × s). The most reasonable value for $\mu'_2/\mu'_1, \mu_2/\mu_1$ is ~ 20, because it corresponds to considerable average tectonic stresses of the order of $\sim 10^2$ MPa (Meissner and Strehlau, 1982; Cloetingh and Wortel, 1985). The values of h_1 and $\tilde{h}_2$ can be also treated in terms of the effective thickness of the high-viscosity (or competent) cores of the crustal and, respectively, mantle parts of the lithosphere (Zuber and Parmentier, 1986; Zuber, 1987). It does not change the relation (eq. 2.1), since the definition of the flexural rigidity D_v for the case of viscous flexure is analogous to that for the elastic case:

$$D_v = \mu_{eff}\left(h_1^3 + \tilde{h}_2^3\right)3n \qquad (2.4a)$$

while for the elastic rigidity D_e, expressed via the effective Young modules E and Poissons's ratio ν, we have:

$$D_e = E\left(h_1^3 + \tilde{h}_2^3\right)/12(1-\nu^2) \qquad (2.4b)$$

This similarity of eqs. (2.4a) and (2.4b) allows us to interpret the estimates of the effective elastic thickness in terms of effective mechanical thickness of high-viscosity crustal and mantle layers.

Gravity anomalies in the Western Gobi region

The crust does not contribute significantly to the total strength of the lithosphere and, therefore, does not significantly affect its overall deflections under distributed vertical loads or point forces (e.g. flexure of lithosphere due to load of surface topography). The crust has, however, to be taken into account in problems of non-uniform horizontal deformation of the lithosphere, because in this case the crustal and mantle lithospheric levels are allowed to deform more independently. Such effects play a potentially important role in the case of folding/buckling of the competent upper crustal layer overlying a low-viscosity lower crust. This process begins due to the application of compressional horizontal stresses at margins of the plate. Because of the presence of the competent crust/viscous crust and viscous crust/mantle interfaces, the competent crust may fold relatively independently of the lithospheric mantle. One of the characteristic features of such process will be the modest expression in the observed Bouguer gravity, whilst the periodical elevations of the basement may be considerable. The main source of Bouguer anomalies is related to deformation of the Moho boundary, which presents the main density discontinuity in the lithosphere. Since there is no significant density change associated with the transition from the mechanically strong upper crust to the underlying low-viscosity crust, deformation of the interface between these layers will be not immediately expressed in the gravity field.

The Western Gobi region (Fig. 2) is characterised by the occurrence of sub-parallel periodically spaced SE–NW-striking folds, which are particularly well expressed on profiles of neotectonic movements of the upper surface (Fig. 4, see

also figs. 2 and 4 in Nikishin et al., 1993-this volume). Spatial spectral analysis detects two dominant harmonics corresponding to wavelengths of about 50 and 300–360 km. Figures 2 and 3 show the location of four data profiles, selected in such a way that they cross the bends of most pronounced folding. Figure 2a,b gives the topography and Bouguer anomaly map of Central Asia with the general location of the profiles, whereas Figures 4 and 5 display the individual profiles. The data profiles include the observed Bouguer gravity anomalies, amplitudes of the vertical neotectonic movements, topography, and the theoretical Bouguer anomalies calculated for a simple model of the local compensation (Airy isostasy). These data reveal the existence of discrepancies of up to 50 mGal between the observed gravity signal and the signal predicted by the "reference" Airy model. This is undoubtedly a significant indication for the existence of a

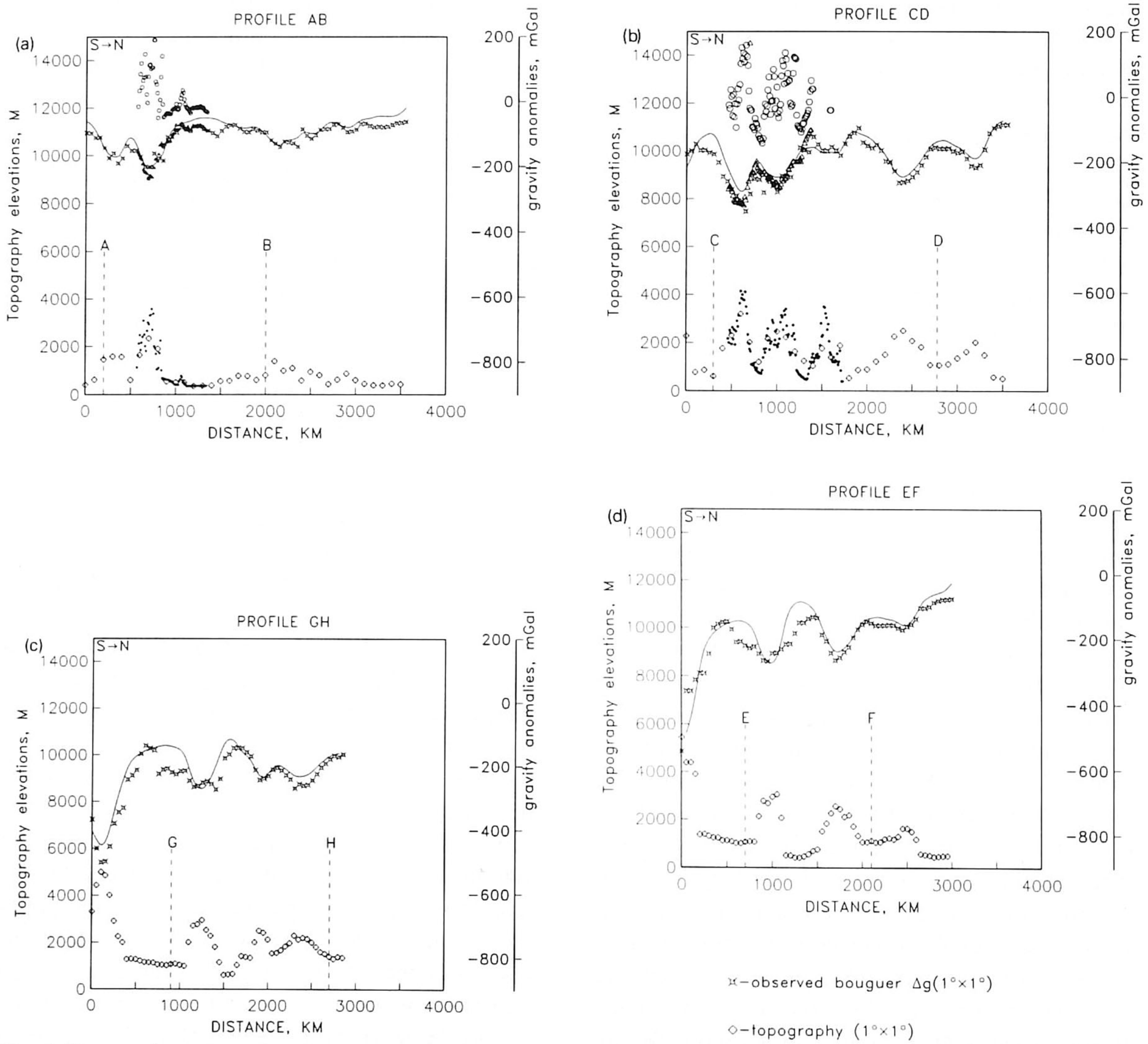

Fig. 5. Topography and gravity data profiles across the Western Gobi. Crossed circles correspond to the observed $60' \times 60'$ Bouguer gravity data (mGal), ◇ = topography (m), thin solid line is the theoretical Bouguer gravity for Airy isostasy (mGal). Filled circles, triangles and open circles correspond to $7.5' \times 5'$ topography, Bouguer and free-air gravity data respectively. (a) Profile *A–B*. Point *A*: 38.5°N, 67.0°E. Point *B*: 50.0°N, 83.0°E. (b) Profile *C–D*. Point *C*: 37.5°N, 68.5°E. Point *D*: 51.0°N, 93.5°E. (c) Profile *G–H*. Point *G*: 41.0°N, 82.5°E. Point *H*: 49.5°N, 101.5°E. (d) Profile *E–F*. Point *E*: 41.0°N, 82.5°E. Point *F*: 50.5°N, 93.5°E.

more complicated mechanism of isostatic compensation. The periodical character of neotectonic movements also points to the presence of some specific dynamic processes responsible for the observed periodicity. The mechanism capable to create such sub-periodical structures is probably related to the mechanism of the dynamic folding of the crustal and mantle layers of the lithosphere due to the horizontal stresses resulting from the northward movement of the Indian plate (Cloetingh and Wortel, 1985, 1986).

Folding of rheologically stratified lithosphere: theory

The theory of the folding of a strong (*competent*) layer surrounded by significantly weaker material has been treated with assumption of various rheologies in series of papers published since the late fifties (Biot, 1957, 1961; Timoshenko and Woinowsky-Krieger, 1959; Sherwin and Chapple, 1968; Ramberg, 1970; Fletcher, 1974, 1977; Smith, 1975, 1977, 1979; Fletcher and Hallet, 1983; Ricard and Froidevaux, 1986; Zuber and Parmentier, 1986; Zuber, 1987; Bird and Gratz, 1990; Marthinod and Davy, 1992). Consider a layered system consisting of a layer of effective viscosity μ_2 surrounded by material of lower viscosity μ_1 and undergoing uniform shortening at a basic strain rate $\dot{\epsilon} \sim (2/L)(\mathrm{d}L/\mathrm{d}t)$, where L is a length of a reference segment. According to the theory of folding, if the layer is much stronger than the surroundings ($\mu_2 \gg \mu_1$), the system as whole becomes unstable and folding of the layer begins (Smith, 1979). The deformations developing during shortening are caused by amplification of small random pre-existing disturbances taking place at the boundaries (interfaces) of the layers. One of the obvious reasons for the origin of the initial "waviness" of the interfaces is the flexural deformation of the lithosphere due to the presence of pre-existing non-uniformly distributed topography loads. The irregularities on the interface between the materials produce a secondary perturbation flow which, in turn, interacts with the interface and deforms it. The intensity of the flow and the amplitude A of the irregularity grow together influencing each other.

The stress components for generalised 2-D case can be expressed as:

$$\sigma_{ij} = -P\delta_{ij} + \mu(\theta)\dot{\epsilon}_{ij} \quad i,j = 1,2$$

$$P = p + \tilde{p};\ \theta = \dot{\epsilon}_{11}^2 + \dot{\epsilon}_{12}^2 + \dot{\epsilon}_{22}^2 = \left(\dot{E}_{11} + \tilde{\dot{\epsilon}}_{11}\right)^2 + \left(\dot{E}_{12} + \tilde{\dot{\epsilon}}_{12}\right)^2 + \left(\dot{E}_{22} + \tilde{\dot{\epsilon}}_{22}\right)^2$$

Here P is the pressure equal to the sum of the basic (p) and perturbation ($\tilde{p}$) pressure components, is the viscosity defined as a function of θ (θ is the second invariant of the strain rate, defined as a sum of the basic strain rate $\dot{E}$ and perturbation strain rate $\dot{\epsilon}$). Let $n_2 = \mu_2/\eta_2$, $n_1 = \mu_1/\eta_1$ be the effective power exponents for the layers (here η_2 and η_1 are the effective viscosities for perturbation normal shear), and γ be the non-dimensional growth rate which depends on the ratio $m = \mu_2/\mu_1$, on n_2, n_1 and on the ratio of the wavelength of the irregularity λ to the layer thickness H. First, let us consider a limit case of strongly non-Newtonian layer ($n_2 \to \infty$) embedded in Newtonian material ($n_1 \to 1$). The perturbation constitutive equations for the layer are (Smith, 1977, 1979):

$$\begin{cases} \sigma_{11} = -P \\ \sigma_{12} = \mu_2\left(\dfrac{\partial u}{\partial y} + \dfrac{\partial v}{\partial x}\right) \\ \sigma_{22} = -P \end{cases} \tag{3.1}$$

The continuity equation is:

$$\frac{\partial u}{\partial y} + \frac{\partial v}{\partial x} = 0$$

The strain rate components are: $\dot{\epsilon}_{11} = 2\ \partial u/\partial x$; $\dot{\epsilon}_{12} = \partial u/\partial y + \partial v/\partial x$; $\dot{\epsilon}_{22} = 2\ \partial v/\partial y$.

Defining the stream function ψ for velocity perturbations $\tilde{v}$ and $\tilde{u}$ ($u = u_0 + \tilde{u}$; $v = v_0 + \tilde{v}$) as:

$$\frac{\partial \psi}{\partial x} = -\tilde{v};\ \frac{\partial \psi}{\partial y} = \tilde{u}$$

we obtain the equilibrium equation:

$$\psi_{xxxx} - 2\psi_{xxyy} + \psi_{yyyy} = 0 \tag{3.1a}$$

with separable solution for ψ:

$$\psi = e^{i\alpha x}\left[C_1 \sin(\alpha y) + C_2 y \sin(\alpha y) + C_3 \cos(\alpha y) + C_4 y \cos(\alpha y)\right] \equiv \Phi_1(y) e^{i\alpha x}$$

For simplicity, we assume here that the surrounding material has the Newtonian ($n_1 \to 1$) rheology (for the lithosphere, due to the strong difference in the characteristic stress relaxation time of the material of the competent layers and surroundings, the rheological "details" of the surroundings, such as power law exponent, are probably not very important). This assumption allows one to rewrite the perturbation constitution and equilibrium equations for the surroundings in the following form:

$$\begin{cases} \sigma_{11} = -P + 2\mu_1 \dfrac{\partial u}{\partial x} \\ \sigma_{12} = \mu_1 \left(\dfrac{\partial u}{\partial y} + \dfrac{\partial v}{\partial x} \right) \\ \sigma_{22} = -P + 2\mu_1 \dfrac{\partial v}{\partial y} \end{cases} \tag{3.2}$$

Equations (3.2) can be reduced to the biharmonic equation:

$$\psi_{xxxx} + 2\psi_{xxyy} + \psi_{yyyy} = 0 \tag{3.2a}$$

The general solution of the equilibrium equation is:

$$\psi = e^{i\alpha x}\left[e^{-\alpha y}\left(\tilde{C}_1 + y\tilde{C}_2\right) + e^{\alpha y}\left(\tilde{C}_3 + y\tilde{C}_4\right)\right] \equiv \Phi_2(y) e^{i\alpha x}$$

Now, to solve eqs. (3.1) and (3.2) together, we assign four boundary conditions acting on the interface between the strong layer and the surrounding material (Smith, 1979):

No slip condition, continuity of horizontal velocity:

$$\tilde{v}_1 = \tilde{v}_2$$

Continuity of vertical velocity:

$$\tilde{u}_1 = \tilde{u}_2$$

Continuity of the tangential stress:

$$\Delta\sigma_{12} = 4(\mu_2 - \mu_1)\frac{1}{L}\frac{dL}{dt}\frac{\partial h}{\partial x}$$

Continuity of normal stress:

$$\Delta\sigma_{22} = 0$$

Assuming also that the local displacement of the interface from its mean position $h(x,t)$ satisfies the *kinematic condition* $\partial h/\partial t = v$, we can rewrite the boundary conditions as:

$$\Phi_1 = \Phi_2$$

$$\frac{\partial \Phi_1}{\partial y} = \frac{\partial \Phi_2}{\partial y}$$

$$\frac{\mu_2}{\mu_1}\left(\frac{\partial^2 \Phi_2}{\partial y^2} + \alpha^2 \Phi_2\right) - \left(\frac{\partial^2 \Phi_1}{\partial y^2} + \alpha^2 \Phi_1\right) = -4\alpha^2 \frac{\left(\dfrac{\mu_2}{\mu_1} - 1\right.}{\gamma} \Phi_1 \tag{3.2b}$$

$$\frac{\mu_2}{\mu_1}\left(\frac{\partial^3 \Phi_2}{\partial y^3} + \frac{\alpha^2\, \partial \Phi_2}{\partial y}\right) = \frac{\partial^3 \Phi_1}{\partial y^3} - \frac{3\alpha^2\, \partial \Phi_1}{\partial y}$$

To simplify the solution, we assume $\psi(x,-y) = -\psi(x,y)$ and the solution for dimensionless growth rate of instability of growth γ (defined as $\gamma \equiv G/(\dot{\epsilon}/2) - 1$; $G = A^{-1} dA/dt$) will be:

$$\gamma = \frac{2m^2 \tan\dfrac{K}{2}}{m + \dfrac{K}{2} + \tan K + \left(m + \dfrac{K}{2}\right)\tan^2\dfrac{K}{2}} \tag{3.3}$$

where $m = \mu_2/\mu_1$ and $K = 2\pi H/\lambda$.

Derivation of the expression for growth rate of folds γ for arbitrary values of μ_2, μ_1, n_2, n_1 (with the only limitation that $\mu_2 > \mu_1$, $n_2 > n_1$, $\mu_2 > \eta_2$, $\mu_1 > \eta_1$) is analogous to the case of ($n_2 \to \infty$; $n_1 \to 1$).

The equilibrium equations (3.1a, 3.2a) will have the following form:

$$\psi_{xxxx} + 2(2/n_{1,2} - 1)\psi_{xxyy} + \psi_{yyyy} = 0$$

whilst the last boundary condition in eq. (3.2b) will be replaced with:

$$\frac{\mu_2}{\mu 1}\left[\frac{\partial^3 \Phi_2}{\partial y^3} - \frac{\alpha^2\, \partial \Phi_2}{\partial y}(4/n_2 - 1)\right] = \frac{\partial^3 \Phi_1}{\partial y^3} - \frac{\alpha^2\, \partial \Phi_1}{\partial y}(4/n_1 - 1) \tag{3.4}$$

Correspondingly, the expression for growth rate γ, valid for arbitrary values of μ_2, μ_1, n_2, n_1 ($\mu_2 > \mu_1$, $n_2 > n_1$, $\mu_2 > \eta_2$, $\mu_1 > \eta_1$), is:

$$\gamma = \frac{2n_2(1-m^{-1})}{Q^2 + \sqrt{n_2 - 1} + \dfrac{(1+Q)^2 e^{Kn_2^{-1/2}} - (1-Q)^2 e^{-Kn_2^{-1/2}}}{2\sin\sqrt{1-n_2^{-1}}\,K}} - 1 \qquad (3.5)$$

where $Q = m^{-1}\sqrt{(n_2/n_1)}$

One can see from eqs. (3.3–3.5) that in the limit case of $m \to \infty$ the growth rate $\gamma \sim \sqrt[3]{m}$. Note also that in the initial stage the growth of folds is governed by more simple relation:

$$\frac{1}{A}\frac{\mathrm{d}A}{\mathrm{d}t} = -\frac{\gamma+1}{L}\frac{\mathrm{d}L}{\mathrm{d}t} \qquad (3.6)$$

The dominant wavelength λ/H, calculated from eq. (3.5) for values of $m \sim 20$–30 and $n_2 \sim 20$, constrained from combined solution of the perturbation constitution and equilibrium equations and eqs. (2.2b,c) and (2.3) is found to be between 4 and 6. This result is confirmed by results of testing eq. (3.5) against arbitrary values of m and n_2 (Figs. 6 and 7). Figure 6 represents a map of dominant wavelengths corresponding to maximum growth rates for a broad range of values of n_2/n_1 and μ_2/μ_1. From this figure it is evident that for μ_2/μ_1 $(\mu'_2/\mu'_1) \leqslant 20$–$30$ and for $n_2/n_1(n'_2/n'_1) \approx 20$ the dominant value of λ/H is about 4–6. As we mentioned in the previous sections, the range of reasonable values for m is limited by $\sim 10 \div 50$, and by $\sim 10 \div 20$ or slightly more for n_2/n_1 ($n_2 = \mu_2/\eta_2$, $n_1 = \mu_1/\eta_1$, with the effective viscosities for longitudinal and normal stresses μ_1, μ_2, η_1, η_2 defined from the expressions for stress and strain rate components). The values of μ_2/μ_1, μ_2/η_2, μ_1/η_1, obtained from the analysis of this section, are within the limits derived in the preceding sections on the base of the rheological properties of lithospheric materials. It should be noted also that values

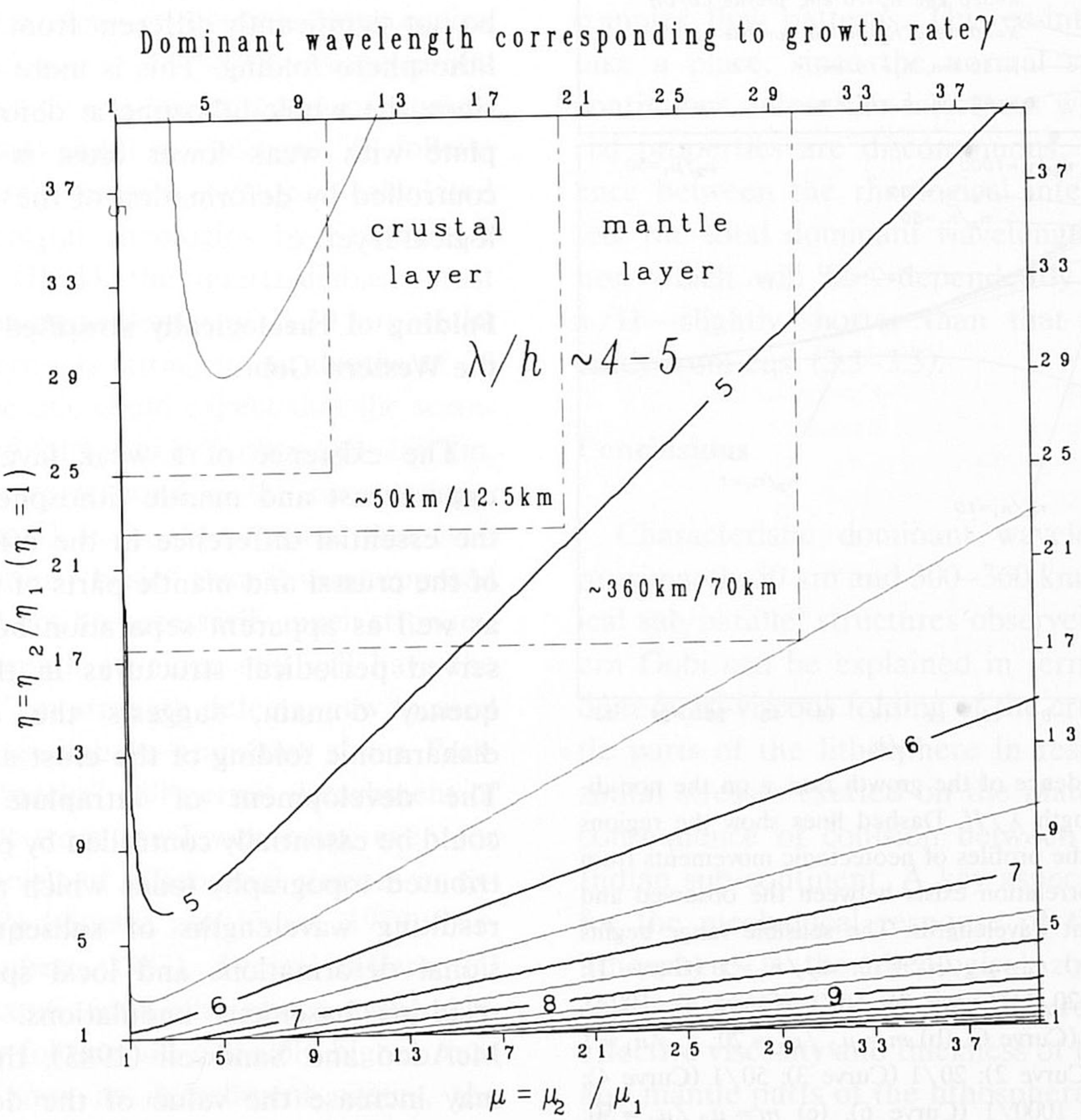

Fig. 6. The map of dominant wavelengths providing maximum growth rates of folds, as a function of n_2/n_1 and μ_2/μ_1. It is clear that for $\mu_2/\mu_1 \leqslant 20$–30 and for $n_2/n_1 \approx 20$ the dominant value of λ/H is about 4.5–6.

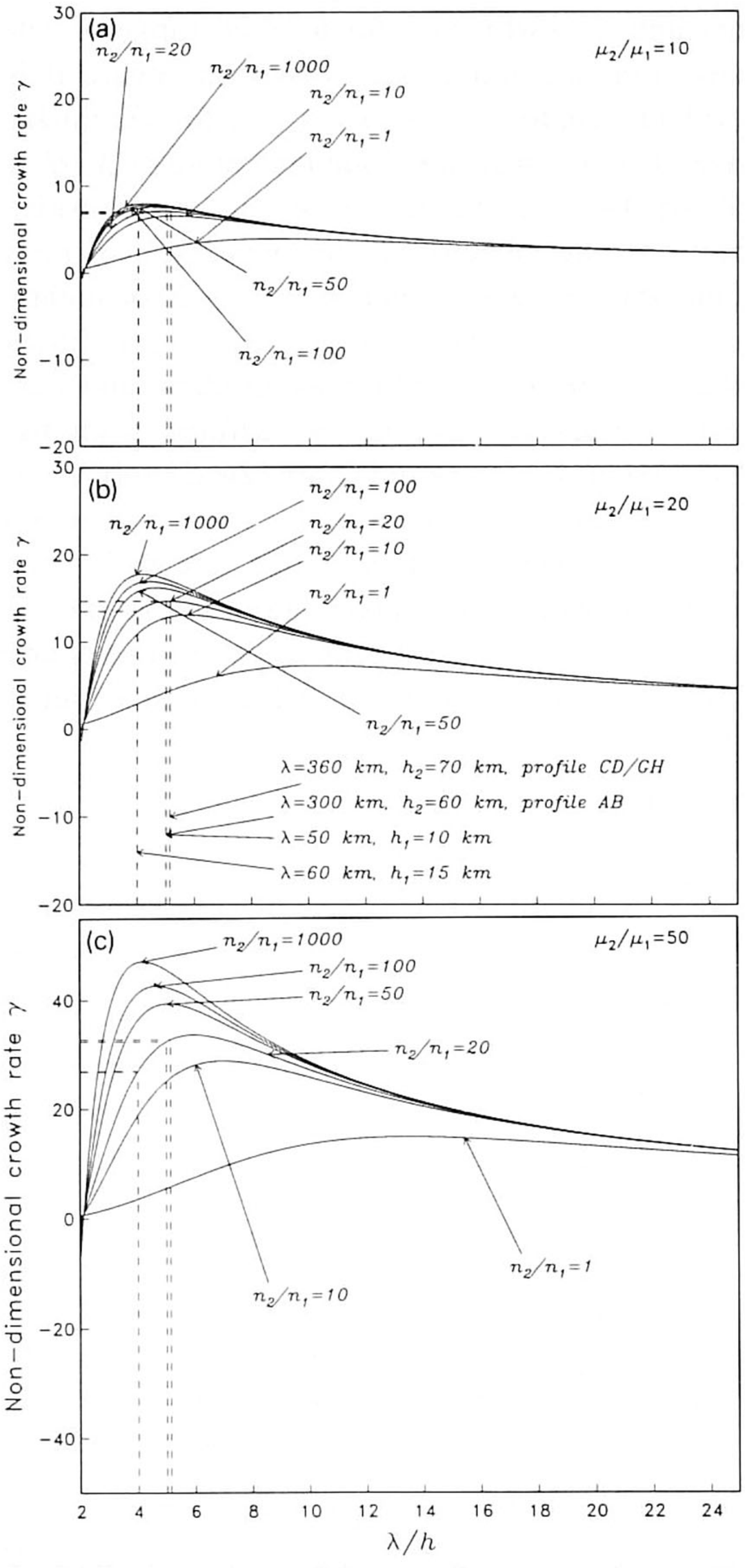

Fig. 7. The dependence of the growth rate γ on the non-dimensional wavelength λ/H. Dashed lines show the regions characteristic for the profiles of neotectonic movements from Fig. 4. A good correlation exists between the observed and predicted dominant wavelengths. The sensible range begins from $\lambda/H \geqslant 2$. (a) $m=\mu_2/\mu_1=10$: $n_2/n_1=1$ (Curve 1); 10/1 (Curve 2); 20/1 (Curve 3); 50/1 (Curve 4); 100/1 (Curve 5); 1000/1 (Curve 6). (b) $m=\mu_2/\mu_1=20$: $n_2/n_1=1$ (Curve 1); 10/1 (Curve 2); 20/1 (Curve 3); 50/1 (Curve 4); 100/1 (Curve 5); 1000/1 (Curve 6). (c) $m=\mu_2/\mu_1=50$: $n_2/n_1=1$ (Curve 1); 10/1 (Curve 2); 20/1 (Curve 3); 50/1 (Curve 4); 100/1 (Curve 5); 1000/1 (Curve 6).

20–30 for m and 20 for n_2/n_1 are in good agreement with earlier estimations made by Smith (1977). Figure 7 shows the growth rate as a function of wavelength λ/H calculated for different values of n_2/n_1 and μ_2/μ_1. The values of the growth rate γ computed for rheological parameters best representing the lithosphere, are in a relatively narrow range of 15–30. Another conclusion drawn on the base of this figure is that the maximum growth rate will be reached at smaller wavelengths as n_2 increases. To consider the whole-lithospheric folding, we solve a system of four sub-systems of equations, analogous to eqs. (3.1) and (3.2), for the upper crust, lower crust, mantle lithosphere and asthenosphere. The boundary conditions are analogous to eqs. (3.2b) and (3.4), and assigned correspondingly at the upper crust, upper crust/lower crust; lower crust/mantle lithosphere, mantle lithosphere/asthenosphere interfaces. The results appear to be not significantly different from that for mantle lithosphere folding. This is more or less obvious since the whole-lithospheric deformation in the plate with weak lower crust is predominantly controlled by deformation of the strongest rheological layer.

Folding of rheologically stratified lithosphere in the Western Gobi

The existence of a weak layer between the upper crust and mantle lithosphere, along with the essential difference in the effective strength of the crustal and mantle parts of the lithosphere as well as apparent separation between the observed periodical structures in the spatial frequency domain, suggests the occurrence of disharmonic folding of the crust and the mantle. The development of intraplate deformations could be essentially controlled by pre-existing distributed topography loads which affect both the resulting wavelengths of subsequent compressional deformations and local spacing between resulting basement undulations. As shown by McAdoo and Sandwell (1985), the initial loads may increase the value of the dominant wavelength of the deformation in the lithosphere. For a thermal age of approximately 500 Ma, a Moho

depth $h \approx 50$ km and a surface heat flow value of ~ 60 mW/m^2, corresponding to the Western Gobi, an estimate for the effective elastic thickness of the competent crust and mantle is about 10–20 km and 65 km, respectively (Burov and Diament, 1992). For these values, the area between the base of the mechanically strong crust and the upper boundary of the mantle lithosphere presents a low-viscosity layer 2–3 times thicker than the strong crust itself. As shown in the previous section, the typical relation between the dominant wavelength of folding and the effective thickness of the competent layer is about 4–6. This supports the notion that the first of the two dominant wavelengths, forming the sub-parallel structures in the Western Gobi region (50 km), is related to folding of the strong high-viscosity upper crustal layer having an effective thickness of about 10–15 km. Structures with a wavelength of 300–360 km are probably caused by folding of the competent mantle layer having an effective thickness of 40–70 km. These results also conform our initial assumption of quartz-dominated crustal rheology, because, as follows from lithosphere strength envelopes calculated for different crustal rheologies by Stephenson and Cloetingh (1991), the quartz-diabase crust should be strong up to depths of > 30 km, whilst quartz-diorite crust is strong up to depths of 25 km. In that case one could expect that the wavelength of related folds will be within 100–180 km, which does not correspond to the observations. On the other hand, it should be noted that even if the crust is more "basic" than it was supposed for Gobi, it will not be necessarily much stronger. The crustal strength envelope still will have the narrow "necks", or strength defects, now located at quartz- diorite- diabase- transition zones. Presence of these "necks" will permit detachment of the upper crust from the lower crust, even for relatively low levels of differential stresses in excess of 100 MPa (Goetze and Evans, 1979; Turcotte and Schubert, 1982). Typical differential stresses in the continental lithosphere, induced by flexure and/or folding are normally higher than 100 MPa. As soon as detachment occurs, the differential motion of the layers will start and facilitate an additional decrease in strength of the detached layers (e.g. heating due to viscous friction).

The topographic loads, disturbing the geometry of the interface between the high-viscosity crust and the underlying low-viscosity crustal channel, will affect the flow of lower-crustal material and may lead to appearance of non-uniform secondary flow "cells". In fact, Smith (1979) has shown that such perturbation "cells" may be induced by irregularities of the shape of the interface between the shearing materials with different viscosities. The continental lithosphere is characterised by at least three interfaces (strong crust–viscous crust–strong mantle lithosphere–viscous mantle lithosphere) along which the shearing movements may take place. If these interfaces are closely spaced (at the distance of order 1/4–1/6), disturbances developing along one interface, may influence deformation along the adjacent interface, resulting in much more complex flow patterns. This co-interaction must take a place, since the normal stress must be continuous across the interfaces while the material properties are discontinuous. Such interflu-ence between the rheological interfaces will affect the total dominant wavelength of deformation which will be—dependently on time and λ/H—slightly shorter than that computed directly from eqs. (3.3–3.5).

Conclusions

Characteristic dominant wavelengths of approximately 50 km and 300–360 km of the periodical sub-parallel structures observed in the Western Gobi can be explained in terms of independent quasi-viscous folding of the crustal and mantle parts of the lithosphere in response to horizontal stresses exerted on the plate margins as a consequence of collision between Asia and the Indian sub-continent. A key aspect of the model for the mechanical response of the continental lithosphere is the rheological zonation of the continental lithosphere. The differentiation in the effective viscosity and thickness of the upper crust and mantle parts of the lithosphere, separated by a low-viscosity layer, is consistent with different wavelengths of folds in the Western Gobi region.

The simple semi-analytical estimates for the dominant wavelengths constrained by the data from experimental rock mechanics, topography, and gravity provide a useful framework for the discussion of the spatial characteristics of large-scale folding of the lithosphere in Central Asia.

Acknowledgements

The authors acknowledge partial funding from the International Lithosphere Project. E. Burov also acknowledges the West–East European Gravity Project (GETECH/University of Leeds), for partial support of this research, and Dr. M.G. Kogan (Institute of Physics of the Earth, Moscow) for useful consultations. Our special thanks go to Prof. G. Ranalli and to the anonymous reviewers for many useful comments on the manuscript. We also thank Prof. P. Molnar (MIT, USA), Prof. M. Diament and Prof. P. Tapponnier (IPGP, France) for helpful discussions.

References

Biot, M.A., 1957. Folding instability of a layered viscoelastic medium under compression. Proc. R. Soc. London A., 242: 444–454.

Biot, M.A., 1961. Theory of folding of stratified viscoelastic media and its implications in tectonics and orogenesis. Geol. Soc. Am. Bull., 72: 1595–1620.

Bird, P. and Gratz, A.J., 1990. A theory for buckling of the mantle lithosphere and Moho during compressive detachments in continents. Tectonophysics, 177: 325–336.

Brace, W.F. and Kohlstedt, D.L. 1980. Limits on lithospheric stress imposed by laboratory experiments. J. Geophys. Res., 85: 6248–6252.

Burov, E.B. and Diament, M., 1992. Flexure of the continental lithosphere with multilayered rheology. Geophys. J. Int., 109: 449–468.

Burov, E.B., Kogan, M.G., Lyon-Caen, H. and Molnar, P., 1990. Gravity anomalies, the deep structure and dynamic processes beneath the Tien Shan. Earth Planet. Sci. Lett., 96: 367–383.

Byerlee, J.D., 1978. Friction of rocks. Pure Appl. Geophys., 116: 615–626.

Carslaw, H.S. and Jaeger, J.C., 1959. Conduction of Heat in Solids. Clarendon, Oxford, 510 pp.

Chamot-Rooke, N. and Le Pichon, X., 1989. Zenisu Ridge: mechanical model of formation. Tectonophysics, 160: 175–193.

Chen, W.P. and Molnar, P., 1983. Focal depths of intra continental earthquakes and their implications for the thermal and mechanical properties of the lithosphere. J. Geophys. Res., 88: 4183–4214.

Cloetingh, S. and Wortel, R., 1985. Regional stress field of the Indian Plate. Geophys. Res. Lett., 12: 77–80.

Cloetingh, S. and Wortel, R., 1986. Stress in the Indo-Australian plate. Tectonophysics, 132: 49–67.

De Rito, R.F., Cozzarelli, F.A. and Hodge, D.S., 1986. A forward approach to the problem of non-linear viscoelasticity and the thickness of the mechanical lithosphere. J. Geophys. Res., 91: 8295–8313.

De Rito, R.F., Moses, T.H., Jr. and Munroe, R.J., 1989. Heat flow and thermotectonic problems of the central Ventura Basin, Southern California. J. Geophys. Res., 94: 681–699.

Fadaie K. and Ranalli, G. 1990. Rheology of the lithosphere in the East African Rift System. Geophys. J. Int., 102: 445–453.

Fletcher, R.C., 1974. Wavelength selection in the folding of a single layer with power law rheology. Am. J. Sci., 274: 1029–1043.

Fletcher, R.C., 1977. Folding of a single viscous layer: exact infinitesimal amplitude solution. Tectonophysics, 39: 593–606.

Fletcher, R.C. and Hallet, B., 1983. Unstable extension of the lithosphere: a mechanical model for basin-and-range structure. J. Geophys. Res., 88: 7457–7466.

Goetze, C. and Evans, B., 1979. Stress and temperature in the bending lithosphere as constrained by experimental rock mechanics. Geophys. J.R. Astron. Soc., 59: 463–478.

Hall, M.K. and Chase, C.G., 1989. Uplift, unbuckling and collapse: flexural history and isostasy of the Wind River Range and Granite Mountains, Wyoming. J. Geophys. Res., 94: 17,581–17,594.

King, J.E., 1986. The metamorphic internal zone of the Wopmay Orogen (Early Proterozoic), Canada: 30 km of structural relief in a composite section based on plunge projection. Tectonics, 5: 973–994.

Kirby, S.H., 1983. Rheology of the lithosphere. Rev. Geophys., 21: 1458–1487.

Kirby, S.H., 1985. Rock mechanics observations pertinent to the rheology of the continental lithosphere and the localisation of strain along shear zones. Tectonophysics, 119: 1–27.

Kirby, S.H. and Kronenberg, A.K., 1987. Rheology of the lithosphere: selected topics. Rev. Geophys., 25: 1219–1244.

Kruse, S., McNutt, M., Phipps-Morgan, J. and Royden, L., 1991. Lithospheric extension near Lake Nevada: a model for ductile flow in the lower crust. J. Geophys. Res., 96: 4435–4456.

Kusznir, N. and Karner, G., 1985. Dependence or the flexural rigidity of the continental lithosphere on rheology and temperature. Nature, 316: 138–142.

Li Fu-Tian, Wu Hua, Liu Jian-hua, Hu Ge, Li Qiang and Qu Ke-xin, 1990. 3-D velocity images beneath the Chinese continent and adjacent regions. Geophys. J. Int., 101: 379–394.

Lobkovsky, L.I., 1988. Scheme of the double-scale double-level

plate tectonics and the intraplate crust deformations. Dokl. Acad. Nauk, 302: 62–67 (in Russian).

Lobkovsky, L.I. and Kerchman, V.I., 1992. A two-level concept of plate tectonics: application to geodynamics. Tectonophysics, 199: 343–374.

Mackwell, S.J., Bai, Q. and Kohlstedt, D.L., 1990. Rheology of olivine and the strength of the lithosphere. Geophys. Res. Lett., 17: 9–12.

Marthinod, J. and Davy, Ph., 1992. Periodic instabilities during compression or extension of the lithosphere: 1. Deformation modes from an analytical perturbation method. J. Geophys. Res., 97: 1999–2014.

McAdoo, D.C. and Sandwell, D., 1985. Folding of oceanic lithosphere. J. Geophys. Res., 90: 8563–8569.

McAdoo, D.C., Martin, C.F. and Polouse, S., 1985. Seasat observations of flexure: evidence for a strong lithosphere. Tectonophysics, 116: 209–222.

McNutt, M. and Menard, H.W., 1982. Constraints on the yield strength in the oceanic lithosphere derived from observations of flexure. Geophys. J.R. Astron. Soc., 59: 4663–478.

McNutt, M., Diament, M. and Kogan, M.G., 1988. Variations of elastic plate thickness at continental thrust belts. J. Geophys. Res., 93: 8825–8838.

Meissner, R. and Strehlau, J., 1982. Limits of stresses in continental crusts and their relation to the depth-frequency distribution of shallow earthquakes. Tectonics, 1: 73–89.

Molnar P. and Deng Qidong, 1984. Faulting associated with large earthquakes and the average rate of deformation in central and eastern Asia. J. Geophys. Res., 89: 6203–6227.

Molnar P. and Tapponnier, P., 1981. A possible dependence of the tectonic strength on the age of the crust in Asia. Earth Planet. Sci. Lett., 52: 107–114.

Nikishin, A.M., Lobkovski, L.I., Cloetingh, S. and Burov, E.B.A.M., 1993. Continental lithosphere folding in Central Asia (Part I): constraints from geological observations. In: S. Cloetingh, W. Sassi and F. Horvath (Editors), The Origin of Sedimentary Basins: Inferences from Quantitative Modelling and Basin Analysis. Tectonophysics, 226: 59–72.

Nikolaev, N.I. (Editor), 1985. The Map of Recent Tectonics of the USSR and Near Regions. Scale 1:400,000. GUGK USSR, Moscow (in Russian).

Parsons, B. and Sclater, J.G., 1977. An analysis of the thermal structure of the plates. J. Geophys.Res., 82: 803–827.

Ramberg, H., 1970. Folding of laterally compressed multilayers in the field of gravity. I. Phys. Earth Planet. Inter., 2: 203–232

Ranalli, G. and Murphy, D.C., 1987. Rheological stratification of the lithosphere. Tectonophysics, 132: 281–295.

Ricard, Y. and Froidevaux, C., 1986. Stretching instabilities and lithospheric boudinage. J. Geophys. Res., 91: 8314–8324.

Sclater, J.G., Jaupart, C. and Galson, D., 1980. The heat flow through oceanic and continental crust and the heat loss of the Earth. Rev. Geophys. Space Phys., 18: 269–311.

Sherwin, J.A. and Chapple, W.M., 1968. Wavelength of single-layer folds: a comparison between theory and observation. Am. J. Sci., 266: 167–179.

Smith, R.B., 1975. Unified theory of the onset of folding, boudinage and mullion structure. Geol. Soc. Am. Bull., 88: 1601–1609.

Smith, R.B., 1977. Formation of folds, boudinage and mullions non-Newtonian materials. Geol. Soc. Am. Bull., 88: 312–320.

Smith, R.B., 1979. The folding of a strongly non-Newtonian layer, Am. J. Sci., 79: 272–287.

Stein, C.A., Cloetingh, S. and Wortel, R., 1989. SEASAT-derived gravity constraints on stress and deformation in the northeastern Indian Ocean. Geophys. Res. Lett., 16: 823–826.

Stephenson, R.A. and Cloetingh, S., 1991. Some examples and mechanical aspects of continental lithospheric folding. Tectonophysics, 188: 27–37.

Tapponnier, P. and Molnar, P., 1979. Active faulting and Cainozoic tectonics of the Tien Shan, Mongolia and Baykal regions. J. Geophys. Res., 84: 3425–3459.

Timoshenko, S.P. and Woinowsky-Krieger, S., 1959. Theory of Plates and Shells. McGraw- Hill, N.Y., 580 p.

Tsenn, M.C. and Carter, N.L., 1987. Flow properties of Continental lithosphere. Tectonophysics, 136: 27–63.

Turcotte, D.L. and Schubert, G., 1982. Geodynamics. Applications of Continuum Physics to Geological Problems. Wiley, New York, NY, 450 pp.

Zoback, M.D., Prescott, W.H. and Krueger, S.W., 1985. Evidence for lower crustal strain localisation in elastic thickness of continental thrust belts. Nature, 317: 7705–7707.

Zuber, M.T., 1987. Compression of oceanic lithosphere: an analysis of intraplate deformation in the Central Indian Basin. J. Geophys. Res., 92: 4817–4825.

Zuber, M.T. and Parmentier, E.M., 1986. Extension of continental lithosphere: a model for two scales of basin and range deformation. J. Geophys. Res., 91: 4826–4838.